DALTON
FULL PAPER

Synthesis and structural characterisation of the isotypic complexes $M^{II}L_2(py)_2\cdot 2H_2O$ (M = Cu, Zn); the interplay of lattice imposed ligand disposition and Jahn–Teller distortions [HL = 5-(4-methoxyphenyl)pyrazole-3-carboxylic acid] †

Jonathan D. Crane,* O. Danny Fox and Ekkehard Sinn *

Department of Chemistry, The University of Hull, Cottingham Road, Kingston-upon-Hull, UK HU6 7RX. E-mail: j.d.crane@chem.hull.ac.uk

Received 19th November 1998, Accepted 17th March 1999

The mononuclear complexes of general formula $ML_2(H_2O)_2$ (M = Zn, Cu, Ni, Co) and $ML_2(py)_2\cdot 2H_2O$ (M = Zn, Cu, Co) have been prepared [HL = 5-(4-methoxyphenyl)pyrazole-3-carboxylic acid, py = pyridine]. The crystal structures of $ZnL_2(py)_2\cdot 2H_2O$ and $CuL_2(py)_2\cdot 2H_2O$ have been determined and are isotypic. Two independent molecules are present in the structures, both of which are pseudo-octahedral with mutually *trans* stereochemistries. In the zinc case the two metal coordination environments differ only slightly and these differences are probably due to packing forces, but for copper the differences are greater and indicate that the direction of the Jahn–Teller distortion observed is dependent upon the subtle constraints imposed by the lattice. The occurrence of such molecular forms is unique for such donor sets and allows a special opportunity to observe the interplay of Jahn–Teller effects and packing forces.

Copper(II) shows great variety and flexibility in its coordination sphere. The ease with which the coordination geometry of copper(II) distorts allows it to adopt commonly a four, five or six coordination number and within the coordination sphere there is also variability in metal–ligand bond lengths.[1] The Jahn–Teller theorem predicts orbitally degenerate copper(II) complexes will distort to remove this degeneracy, resulting in the axially elongated geometry commonly observed for six coordinate copper(II). Such octahedral complexes would be expected to oscillate dynamically between the three possible elongations of mutually *trans* ligands, but typically one of these distortions is dominant and the classic '4 + 2' geometry (four short equatorial and two long tetragonal distances) is observed. An apparent '2 + 4' coordination (axial compression) is due to static/dynamic disorder of two of the possible axial elongations.[2] For an octahedral copper(II) centre with a non-degenerate orbital ground state, due to the low symmetry provided by a non-equivalent donor set, a pseudo-Jahn–Teller distortion would still be expected. The removal of degeneracy provided by a lowering from octahedral symmetry does not separate the levels sufficiently to prevent the copper(II) centre showing a significant distortion.[3]

With a non-equivalent donor set it cannot be predicted in general which metal ligand axis or axes will experience an elongation. If the difference in energy minima between the three possible elongations is low then the stability provided by crystal packing forces may ultimately determine the distortion. The relative strength/basicity of donor ligands[4] and steric control, provided for example by the use of chelating ligands, will further influence the direction of the metal–ligand bond distortion.

The use of X-ray crystallography has been the subject of scrutiny regarding its use as a technique for the determination of Jahn–Teller distortions in metal complexes.[5] Experimentally determined high crystallographic symmetry has been attributed to disorder along the direction of the metal–ligand bonds. In particular it has been suggested that some room temperature determinations may give time averaged structures.[6] For this reason crystallographic evidence purporting to show the absence of a Jahn–Teller distortion must be treated with caution, and the crystallographic determination of the amount of distortion should also be examined critically, especially in high symmetry cases, because the result may be the time average of more than one structure, for which the relative contributions are unknown. However, the presence of static/dynamic disorder of two or more structures can be identified by comparing the components of the anisotropic displacement parameters (U) for the copper atom and the ligand donor atom along the M–X bond.[7]

The nature of the pseudo-Jahn–Teller distortion in *trans*-diaquabis(methoxyacetato)copper(II) has been recently reported at a selection of temperatures over the range 4.2–325 K.[8] The apparent tetragonal compression (short Cu–carboxylate distance) at room temperature is described as a planar dynamic Jahn–Teller system which upon cooling converts to a static tetragonal elongation (long Cu–methoxy distance). In this case the corresponding nickel(II) complex is isostructural and at room temperature has a nearly regular octahedral coordination, whereas the zinc(II) complex adopts the alternative *cis*-diaqua structure.

The coordination chemistry of chelating carboxyl substituted nitrogen heterocycles, *e.g.* 2-pyridinecarboxylic acid, 2-piperidinecarboxylic acid and 2-quinolinecarboxylic acid have been studied for their possible roles as ligands in biological systems.[9] The pyrazole ring has been widely employed as a ligand in bioinorganic model complex systems such as the family of poly(pyrazolyl)borate compounds,[10] and more recently as the bridging group for studies on binuclear metal complexes.[11] In this paper we report the synthesis of the bidentate 5-(4-methoxyphenyl)pyrazole-3-carboxylic acid (HL) and its reaction with the divalent transition metals (Co, Ni, Cu, Zn) to yield mononuclear complexes. A comparison between the crystal structure of the copper(II) complex exhibiting Jahn–Teller distortions and the isostructural and isomorphous zinc(II) complex is discussed.

† *Supplementary data available*: X-ray powder diffraction patterns. For direct electronic access see http://www.rsc.org/suppdata/dt/1999/1461/, otherwise available from BLDSC (No. SUP 57519, 2 pp.) or the RSC Library. See Instructions for Authors, 1999, Issue 1 (http://www.rsc.org/dalton).

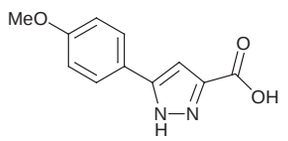

HL

Experimental

All commercial reagents and solvents were used as supplied. IR spectra were recorded using a Perkin-Elmer 983G instrument, ^{1}H NMR spectra on a JEOL-270 (270 MHz) spectrometer and mass spectra on a Finnigan 1020 (electron impact). Diffuse reflectance electronic spectra were recorded on a Cary 5E spectrometer as powders ground with $BaSO_4$ in the ranges 4000 to 40000 cm^{-1}. Elemental analyses were performed using a Fisons Instruments EA 1108 CHN elemental analyser. Room temperature magnetic moments were measured with a Johnson Matthey magnetic susceptibility balance calibrated with Hg[Co(NCS)$_4$], and diamagnetic corrections were experimentally determined from the appropriate zinc(II) complex. X-Ray powder diffraction data were collected on a Philips PW1130 diffractometer using Cu-Kα radiation (1.5 Å).

Syntheses

Ethyl 5-(4-methoxyphenyl)pyrazole-3-carboxylate. To a solution of sodium ethoxide, prepared by dissolving sodium (12 g, 0.52 mol) in ethanol (500 cm^3), was added diethyl oxalate (67.3 cm^3, 0.5 mol) followed by 4-methoxyacetophenone (75 g, 0.5 mol) and the mixture stirred at room temperature (12 h). During this time the sodium salt of the intermediate β-diketonate condensation product precipitated as a thick yellow paste. Sodium hydroxide (21 g, 0.525 mol), hydrazinium sulfate ($N_2H_6SO_4$, 65 g, 0.5 mol) and water (250 cm^3) were added and the mixture stirred (6 h). The cream product was isolated by filtration and recrystallised from ethanol–water (yield 75 g, 61%), mp 154 °C (Found: C, 63.62; H, 5.62; N, 11.31. $C_{13}H_{14}N_2O_3$ requires C, 63.40; H, 5.73; N, 11.38%); ν_{max}/cm^{-1} (KBr disc) 1721s (CO); δ_H($CDCl_3$) 7.62 (2H, d, aryl CH), 6.91 (1H, s, pyrazole CH), 6.89 (2H, d, aryl CH), 4.23 (2H, q, J = 7.0 Hz, $CO_2CH_2CH_3$), 3.81 (3H, s, OCH_3), 1.24 (3H, t, J = 7.0 Hz, $CO_2CH_2CH_3$); *m*/*z* (electron impact) 246 (M^+).

5-(4-Methoxyphenyl)pyrazole-3-carboxylic acid (HL). A solution of ethyl 5-(4-methoxyphenyl)pyrazole-3-carboxylate (10 g, 0.041 mol) and potassium hydroxide (5.2 g, 0.093 mol) in water (300 cm^3) was heated under reflux (2 h), then allowed to cool to room temperature. Acidification with dilute hydrochloric acid (2 M) afforded HL as a white solid, which was filtered off and oven dried (8.93 g, 93%), mp 225 °C (decomp.) (Found: C, 60.53; H, 4.45; N, 12.82. $C_{11}H_{10}N_2O_3$ requires C, 60.55; H, 4.62; N, 12.84%); ν_{max}/cm^{-1} (KBr disc) 1674s (CO), 1250s; δ_H(CD_3OD) 7.65 (2H, d, aryl CH), 6.96 (2H, d, aryl CH), 6.99 (1H, s, pyrazole CH), 3.79 (3H, s, OCH_3); δ_H(dmso) 12.5 (s, pyrazole NH and CO_2H), 7.75 (2H, m, aryl CH), 6.97 (2H, m, aryl CH), 6.94 (1H, s, pyrazole CH), 3.78 (3H, s, OCH_3); *m*/*z* (electron impact) 218 (M^+).

Preparation of the $ML_2(H_2O)_2$ complexes

$ZnL_2(H_2O)_2$ 1. HL (1.0 g, 4.6 mmol) and $Zn(OAc)_2{\cdot}2H_2O$ (0.5 g, 2.3 mmol) were heated in water (200 cm^3, 4 h, 80 °C) with stirring. The resultant white precipitate of **1** was filtered off and dried *in vacuo* (0.97 g, 79%) (Found: C, 48.96; H, 3.88; N, 10.19. $C_{22}H_{22}N_4O_8Zn$ requires C, 49.32; H, 4.14; N, 10.46%); ν_{max}/cm^{-1} (KBr disc) 3113br (OH), 1609s (CO), 1412s, 840, 699; δ_H(dmso) 13.7 (2H, br s, NH), 7.79 (4H, d, aryl CH), 6.99 (4H, aryl CH), 6.94 (2H, s, pyrazole CH), 3.79 (6H, s, OCH_3).

$CuL_2(H_2O)_2$ 2. The green precipitate from water obtained by mixing HL and $Cu(OAc)_2{\cdot}2H_2O$ as described above was recrystallised from dmf–water as a powder (1.05 g, 85%) (Found: C, 49.08; H, 4.04; N, 10.36. $C_{22}H_{22}CuN_4O_8$ requires C, 49.48; H, 4.15; N, 10.49%); ν_{max}/cm^{-1} (KBr disc) 3369br (OH), 1657s (CO), 1423s, 834, 775; λ_{max}/cm^{-1} (diffuse reflectance) 14700, 25000 (sh), 28600; μ_{eff} = 1.85 μ_B.

$NiL_2(H_2O)_2$ 3. The light blue powder obtained by mixing HL and $Ni(OAc)_2{\cdot}4H_2O$ as described above was recrystallised from dmf–water (1.05 g, 86%) (Found: C, 49.55; H, 4.03; N, 10.47. $C_{22}H_{22}N_4NiO_8$ requires C, 49.94; H, 4.19; N, 10.59%); ν_{max}/cm^{-1} (KBr disc) 3207br (OH), 1634s (CO), 1423s, 830, 776; λ_{max}/cm^{-1} (diffuse reflectance) 8400, 15800, 25300; μ_{eff} = 3.26 μ_B.

$CoL_2(H_2O)_2$ 4. The pale orange powder obtained by mixing HL and $Co(OAc)_2{\cdot}4H_2O$ as described above was recrystallised from dmf–water (0.82 g, 68%) (Found: C, 49.99; H, 4.12; N, 10.54. $C_{22}H_{22}N_4CoO_8$ requires C, 49.92; H, 4.19; N, 10.58%); ν_{max}/cm^{-1} (KBr disc) 3206br (OH), 1614s (CO), 1417s, 1251s, 1024, 828; λ_{max}/cm^{-1} (diffuse reflectance) 8200, 21500, 26100; μ_{eff} = 4.77 μ_B.

Preparation of the $ML_2(py)_2{\cdot}2H_2O$ complexes

$ZnL_2(py)_2{\cdot}2H_2O$ 5. The slow evaporation of a solution of **1** in pyridine yielded colourless X-ray quality crystals of **5** (Found: C, 55.79; H, 4.45; N, 11.99. $C_{32}H_{32}N_6O_8Zn$ requires C, 55.37; H, 4.65; N, 12.11%); ν_{max}/cm^{-1} (KBr disc) 3122br (OH), 1638s (CO), 1412s, 698; δ_H(dmso) 13.7 (1.5H, br s, NH), 8.59 (4H, pyridine H_{ortho}), 7.80 (6H, m, overlapped pyridine H_{para} and aryl CH), 7.42 (4H, pyridine H_{meta}), 7.00 (6H, m, overlapped aryl CH and pyrazole CH), 3.77 (6H, s, OCH_3).

$CuL_2(py)_2{\cdot}2H_2O$ 6. Diffusion of water vapour into a solution of **2** in pyridine yielded large, X-ray quality, green crystals of **6** (Found: C, 55.53; H, 4.66; N, 12.14. $C_{32}H_{32}N_6CuO_8$ requires C, 55.52; H, 4.60; N, 12.27%); ν_{max}/cm^{-1} (KBr disc) 3122br (OH), 1641s (CO), 1416s, 847, 796, 697; λ_{max}/cm^{-1} (diffuse reflectance) 14700, 25000 (sh), 28500.

$CoL_2(py)_2{\cdot}2H_2O$ 7. Diffusion of water vapour into a solution of **4** in pyridine yielded orange crystals of **7** (Found: C, 56.46; H, 4.75; N, 12.45. $C_{32}H_{32}CoN_6O_8$ requires C, 55.90; H, 4.69; N, 12.22%); ν_{max}/cm^{-1} (KBr disc) 3410br (OH), 1630s (CO), 1412s, 1299s, 699; ν_{max}/cm^{-1} (diffuse reflectance) 9100, 21000, 25600.

Crystallography

The X-ray work was carried out as previously described,[12,13] using a Rigaku AFC6S diffractometer with graphite monochromated Mo-Kα radiation on crystals mounted on glass fibres using epoxy resin. Details of the experimental conditions and structure refinement data are listed in Table 1. The intensities of three representative reflections which were measured after every 150 reflections declined by −1.10% for **5** and 11.0% for **6**. A linear correction factor was applied to the data to account for this phenomenon. Lorentz polarisation corrections and an empirical absorption correction based on azimuthal scans of several reflections, was applied which resulted in transmission factors ranging from 0.73 to 1.22 for **5** and 0.76 to 1.21 for **6**.

CCDC reference number 186/1392.

Results and discussion

Synthesis and characterisation of the ligand HL and its complexes

The condensation of hydrazinium sulfate with the sodium salt of the β-diketoester formed by the reaction of 4-methoxyacetophenone with diethyl oxalate in the presence of sodium ethoxide yielded the compound ethyl 5-(4-methoxyphenyl)-

Table 1 Crystal and X-ray structure information for complexes **5** and **6**

	5	**6**
Formula	$C_{32}H_{32}N_6O_8Zn$	$C_{32}H_{32}N_6CuO_8$
Molecular weight	694.02	692.19
Space group	$P2_1/n$	$P2_1/n$
a/Å	14.127(5)	14.183(3)
b/Å	12.350(3)	12.551(5)
c/Å	18.565(3)	18.234(6)
β/°	100.55(2)	100.94(3)
Z	4	4
V/Å^3	3184	3187
μ/cm^{-1}	8.46	7.43
T/K	295	296
No. unique reflections measured	8483	4812
No. unique reflections used ($I > 2.5\sigma(I)$)	3051	—
No. unique reflections used ($I > 3.0\sigma(I)$)	—	2070
R, R_w	0.045, 0.044	0.055, 0.055

pyrazole-3-carboxylate. Hydrolysis of this pyrazole ester with aqueous potassium hydroxide and subsequent acidification afforded the ligand 5-(4-methoxyphenyl)pyrazole-3-carboxylic acid (HL) in good overall yield. The divalent transition metal complexes $ML_2(H_2O)_2$ (M = Zn, Cu, Ni, Co) were prepared by reaction of HL with the corresponding metal acetate salt in water. Recrystallisation from pyridine afforded the complexes $ML_2(py)_2{\cdot}2H_2O$ (M = Zn, Cu, Co). The nickel(II) complex **3** was insoluble in pyridine and thus the pyridine derivative could not be prepared. The crystals of $ZnL_2(py)_2{\cdot}2H_2O$ **5** and $CuL_2(py)_2{\cdot}2H_2O$ **6** were of sufficient quality to allow the determination of their structures by X-ray crystallography.

Structures of $ZnL_2(py)_2{\cdot}2H_2O$ 5 and $CuL_2(py)_2{\cdot}2H_2O$ 6

The X-ray crystal structure determinations of these complexes showed both to crystallise in the monoclinic space group $P2_1/n$, *i.e.* the compounds are isotypic. In both structures the metal occupies two unique positions in the unit cell with the two unique sites each possessing $\bar{1}$ symmetry. ORTEP diagrams of the two metal sites of **6** are illustrated in Fig. 1.[14] The disposition of the ligands around each unique metal atom for the zinc and copper structures are superficially the same, however, the distortions of the coordination spheres are different. The metal–ligand bond distances and bond angles for both pairs of metal geometries are summarised in Figs. 1 and 2. The two unique zinc centres in **5** have no significant difference in their Zn–N(pz) bond lengths (pz = pyrazolyl group), 2.063(4) and 2.073(4) Å, and their Zn–O bond lengths, 2.123(4) and 2.136(4) Å. However, there is a markedly larger difference between the Zn–N(py) bonds, 2.270(5) and 2.186(5) Å (difference = 0.084 Å) for Zn(1) and Zn(2) respectively. The chelation of the bidentate pyrazole carboxylate ligand is expected to influence the bond lengths to the zinc, resulting in the Zn–N(py) bonds being the weakest and longest, and most susceptible to crystal packing effects. It is reasonable to attribute the relatively small differences in the two zinc coordination geometries to lattice forces.

In contrast to the zinc centres in **5**, the coordination geometries of the two unique copper centres in **6** are significantly different, with each copper demonstrating a different apparent distortion: Cu(1) has a small elongation along the Cu–N(py) axis whereas Cu(2) has a pronounced elongation along the Cu–O axis. In both cases the Cu–N(pz) bond is the shortest at 1.978(7) and 1.988(7) Å respectively. The Cu(2) site clearly displays the classic '4 + 2' coordination geometry expected of a metal centre experiencing a pseudo-Jahn–Teller distortion. The short Cu(2)–N(pz) [1.988(7) Å] and Cu(2)–N(py) [2.037(7) Å] bonds contrast markedly with the elongated Cu(2)–O bonds [2.355(5) Å]. The chelate effect, which is expected to favour a short Cu–O bond, appears ineffective in the coordination

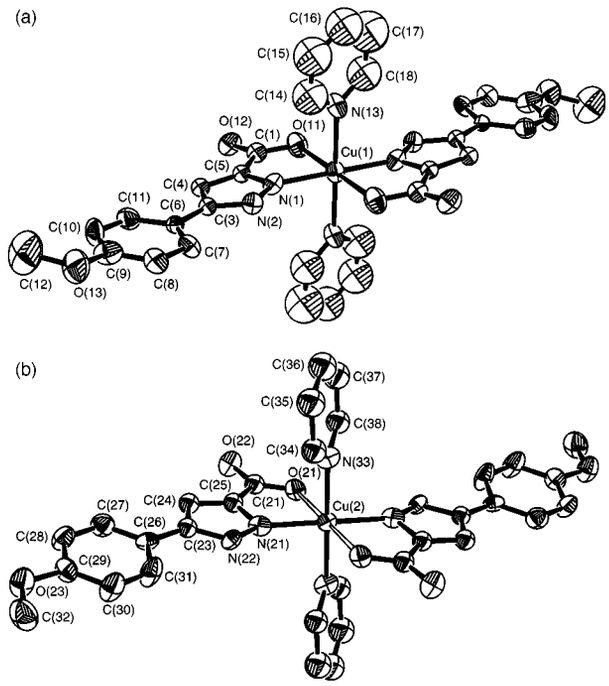

Fig. 1 ORTEP diagrams for the two unique molecules of **6** (probability level 50%).[14] The metal atoms lie on a crystallographic site of $\bar{1}$ symmetry. Selected bond lengths are shown in Fig. 2. Bond angles/°, with e.s.d.s in parentheses: **5** O(11)–Zn(1)–N(1) 78.3(2), O(11)–Zn(1)–N(1′) 101.7(2), O(11)–Zn(1)–N(13) 93.3(2), O(11)–Zn(1)–N(13′) 86.7(2), N(1)–Zn(1)–N(13) 91.3(2), N(1)–Zn(1)–N(13′) 88.7(2), O(21)–Zn(2)–N(21) 78.5(2), O(21)–Zn(2)–N(21′) 101.5(2), O(21)–Zn(2)–N(33) 92.5(2), O(21)–Zn(2)–N(33′) 87.5(2), N(21)–Zn(2)–N(33) 91.1(2), N(21)–Zn(2)–N(33′) 88.9(2); **6** O(11)–Cu(1)–N(1) 77.8(2), O(11)–Cu(1)–N(1′) 102.2(2), O(11)–Cu(1)–N(13) 92.9(3), O(11)–Cu(1)–N(13′) 87.1(3), N(1)–Cu(1)–N(13) 92.0(3), N(1)–Cu(1)–N(13′) 88.0(3), O(21)–Cu(2)–N(21) 76.3(2), O(21)–Cu(2)–N(21′) 103.7(2), O(21)–Cu(2)–N(33) 92.3(2), O(21)–Cu(2)–N(33′) 87.7(2), N(21)–Cu(2)–N(33) 90.2(3), N(21)–Cu(2)–N(33′) 89.8(3).

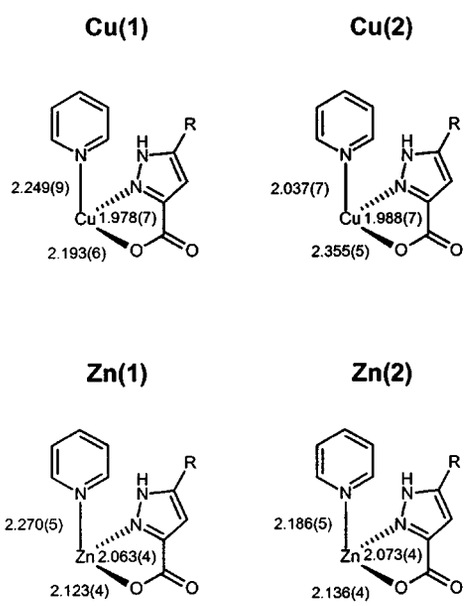

Fig. 2 Schematic diagram illustrating the bond lengths around the two unique metal atoms of the zinc and copper structures **5** and **6** respectively. All metal atoms lie on a crystallographic site of $\bar{1}$ symmetry.

sphere of Cu(2). For the Cu(1) site a clear cut tetragonal distortion is not evident. There is a small elongation along the Cu(1)–N(py) axis [2.249(9) Å], but it is not greater than the elongation observed for the corresponding Zn(1) site [2.270(5) Å]. In addition to the long Cu(1)–N(py) bonds, the long

Table 2 Difference displacement parameters ΔU_{obs} [15] for **5** and **6**, with e.s.d.s in parentheses

M–X	**5** ΔU_{obs}(Zn–X) [a]	**6** ΔU_{obs}(Cu–X) [a]	ΔU(Cu–X)$_{JT}$ [b]
M(1)–O(11)	4 (30)	318 (55)	314 (63)
M(1)–N(1)	2 (31)	79 (55)	77 (63)
M(1)–N(13)	124 (43)	214 (76)	90 (87)
M(2)–O(21)	37 (29)	23 (43)	−14 (52)
M(2)–N(21)	10 (38)	96 (55)	86 (69)
M(2)–N(33)	45 (38)	81 (55)	36 (69)

[a] $\Delta U_{obs}(M–X) = |U(M) - U(X)|$ in Å^2 ($\times 10^4$) evaluated along M–X bonds. [b] $\Delta U(Cu–X)_{JT} = \Delta U_{obs}(Cu) - \Delta U_{obs}(Zn)$.

Cu(1)–O bonds [2.193(6) Å] of the Cu(1) centre represent an environment more akin to a '2 + 4' coordination geometry. However, the overall similarity of the Cu(1) and Zn(1) site structures discounts the possibility that Cu(1) is a rare example of a '2 + 4' tetragonal compressed coordination,[5] or an elongated rhombic octahedral distortion resulting from a pseudo-Jahn–Teller effect.[2] The nature of the distortion of Cu(1) is revealed by considering the ΔU_{obs} values along the Cu–X bonds (Table 2).[7,15] The large values of ΔU_{obs} for Cu(1)–O(11) and Cu(1)–N(33) clearly indicate a case of static/dynamic disorder of two axial elongations along these bonds. Interestingly, the value of ΔU_{obs} for Zn(1)–N(33) is almost as large as for Cu(1), indicating that this pyridine ligand is not tightly constrained by either the metal ion or the lattice for both structures. The small and similar ΔU_{obs} values for Cu(2) and Zn(2) confirm that Cu(2) displays a straightforward elongation of Cu(2)–O(21). Crystal packing forces are probable determining factors for the observation of a single Jahn–Teller distortion of the Cu(2) centre, whereas the presence of two static/dynamic disordered distortions produce the apparent compressed tetragonal structure of the Cu(1) centre.

In the lattice the two complexes are arranged alternately in hydrogen-bonded ribbons (Fig. 3). Hydrogen-bonding to the carboxylate groups could reasonably be expected to be one of the factors influencing the two metal coordination geometries. Based simply upon bond lengths the hydrogen-bonding to coordinated carboxyl oxygens does not appear to perturb the M–O bonds. It therefore appears unlikely that the hydrogen-bonding effects of the occluded water molecules affect the coordination sphere bond lengths of the metals to any great extent.

Spectroscopic characterisation of the complexes

The X-ray powder diffraction patterns of the zinc **1** and nickel **3** complexes are almost identical and these compounds are probably isostructural. There is also a strong similarity between these two compounds and the copper complex **2**. The pattern for the cobalt complex **4** is somewhat different.

The ν_{as} and ν_s stretching modes of the carboxyl group for these complexes (Table 3) are broadly similar to the values reported for the analogous pyridazine-3-carboxylate complexes [16] and *trans* square planar amino acid complexes.[17] In all cases the values of $\Delta\nu$ indicate the presence of monodentate carboxylate ligands. Furthermore, although two different geometries of M–carboxyl bonding occur in **5** and **6**, only one set of IR bands is observed for each compound. For compounds **5**, **6** and **7** the presence of the pyridine molecules is confirmed by the strong absorption at 698 ± 1 cm^{-1}.

The ^{1}H NMR spectrum of $ZnL_2(H_2O)_2$ **1** in dmso contains the expected peaks for the ligand, but shifted compared with the uncomplexed ligand HL. There is only one signal for water and this occurs at the usual position for free water in dmso. The ^{1}H NMR spectrum of $ZnL_2(py)_2{\cdot}2H_2O$ **5** in dmso has an additional three signals for the pyridine molecules and these occur at the same positions as for free pyridine in dmso; the addition of pyridine to this solution also produces no extra peaks. The conclusion for both complexes is that the zinc(II) ion rapidly loses/exchanges its axial ligands upon dissolution in dmso, but that the chelating pyrazole carboxylate ligands probably remain coordinated.

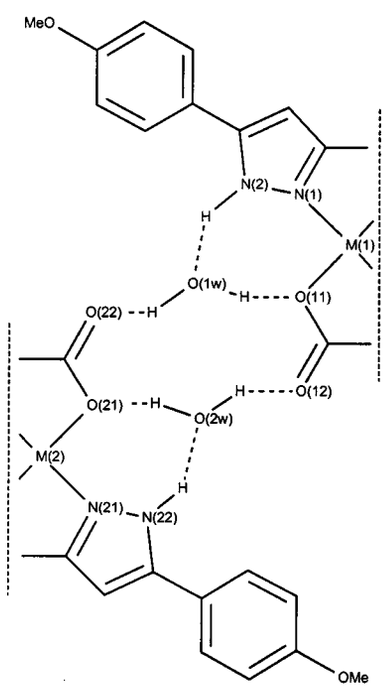

Fig. 3 The hydrogen-bonding network between molecule 1, molecule 2 and the two occluded water molecules for **5** and **6**. Hydrogen bonding distances/Å, with e.s.d.s in parentheses: **5**, O(1W)–O(22) 2.708(5), O(1W)–N(2a) 2.663(5), O(1W)–O(11b) 2.755(5), O(2W)–O(21) 2.858(5), O(2W)–N(22c) 2.751(5), O(2W)–O(12b) 2.831(5); **6**, O(1W)–O(22) 2.655(8), O(1W)–N(2a) 2.655(9), O(1W)–O(11b) 2.712(8), O(2W)–O(21) 2.742(8), O(2W)–N(22c) 2.769(8), O(2W)–O(12b) 2.839(8). Symmetry operations: a, $x - \frac{1}{2}, \frac{1}{2} - y, z - \frac{1}{2}$; b, $\frac{1}{2} - x, y - \frac{1}{2}, \frac{3}{2} - z$; c, $1 - x, 1 - y, 1 - z$.

Table 3 IR spectra (KBr disc) of HL and metal complexes

Compound	$\nu_{as}(CO_2)$/ cm^{-1}	$\nu_s(CO_2)$/ cm^{-1}	$\Delta\nu(CO_2)$ [a]/ cm^{-1}	$\nu(OH_2)$/ cm^{-1}
HL	1674	1250	424	
$ZnL_2(H_2O)_2$ **1**	1609	1412	197	3400
$CuL_2(H_2O)_2$ **2**	1657	1423	234	3369
$NiL_2(H_2O)_2$ **3**	1634	1423	210	3207
$CoL_2(H_2O)_2$ **4**	1614	1417	197	3206
$ZnL_2(py)_2{\cdot}2H_2O$ **5**	1638	1412	226	3370
$CuL_2(py)_2{\cdot}2H_2O$ **6**	1641	1416	215	3400
$CoL_2(py)_2{\cdot}2H_2O$ **7**	1630	1412	218	3410

[a] $\Delta\nu(CO_2) = \nu_{as}(CO_2) - \nu_s(CO_2)$.

The solid state reflectance spectra of the metal complexes all exhibit very strong absorption in the 30000 cm^{-1} region due to charge transfer and/or ligand absorption bands. No other absorptions were detected for the zinc complexes **1** and **5**. The reflectance spectra of the copper complexes **2** and **6** are virtually identical; both show a strong, broad band at 14700 cm^{-1}. Although further detail may be expected due to a tetragonal splitting of the e_g level, none was observed. The degree of similarity between the spectra of **2** and **6** strongly suggests **2** is also six coordinate but with axial water molecules. There is no absorption at 20000 cm^{-1} indicative of a square planar coordination for the copper(II) ion.[18] The reflectance spectrum and magnetic moment of $NiL_2(H_2O)_2$ **3** are typical of an octahedral nickel(II) complex. Three absorptions are

observed at 8400, 15800 and 25300 cm^{-1} and the magnetic moment is 3.26 μ_B. The complex $CoL_2(H_2O)_2$ **4** exhibits the expected reflectance spectrum for an octahedral cobalt(II) ion with absorption bands at 8200, 21500 and 26100 cm^{-1}, however, the experimentally determined magnetic moment of 4.77 μ_B is slightly low for an octahedral cobalt(II) complex.[19] The reflectance spectrum of $CoL_2(py)_2{\cdot}2H_2O$ **7** is almost identical to that of **4** indicating the cobalt(II) in complex **7** is also six coordinate.

Conclusion

The presence of two independent molecules in the structures of $ZnL_2(py)_2{\cdot}2H_2O$ **5** and $CuL_2(py)_2{\cdot}2H_2O$ **6** has allowed a study of packing forces upon coordination geometry in the zinc case, and of the combined effects of packing forces and Jahn–Teller distortions in the copper case. Although the Zn(1) and Zn(2) coordination environments differ only slightly the corresponding copper geometries are markedly different, indicating that for copper(II) subtle differences in lattice constrained ligand disposition can cause much larger differences in the metal coordination environment; Cu(1) displays an apparent tetragonal compression caused by the static/dynamic disorder of two Jahn–Teller tetragonal elongation distortions whereas Cu(2) displays a single Jahn–Teller tetragonal elongation.

Acknowledgements

We thank the EPSRC (studentship to O. D. F.) and the University of Hull for supporting this work.

References

1 J. Gazo, I. B. Bersuker, J. Garaj, M. Kabešová, J. Kohout, H. Langfelderová, M. Melník, M. Serátor and F. Valach, *Coord. Chem. Rev.*, 1976, **19**, 253; I. B. Bersuker, *Coord. Chem. Rev.*, 1974, **14**, 357.
2 L. R. Falvello, *J. Chem. Soc.*, *Dalton Trans.*, 1997, 4463; B. J. Hathaway, in *Comprehensive Coordination Chemistry*, eds. G. Wilkinson, R. D. Gillard and J. A. McCleverty, Pergamon, Oxford, 1988, vol. 5, pp. 690–694.
3 C. J. Simmons, B. J. Hathaway, K. Amornjarusiri, B. D. Santarsiero and A. Clearfield, *J. Am. Chem. Soc.*, 1987, **109**, 1947.
4 F. A. Cotton, L. M. Daniels and C. A. Murillo, *Polyhedron*, 1992, **11**, 2475.
5 D. A. Tucker, P. S. White, K. L. Trojan, M. L. Kirk and W. E. Hatfield, *Inorg. Chem.*, 1991, **30**, 823; P. J. Ellis, H. C. Freeman, M. A. Hitchman, D. Reinen and B. Wagner, *Inorg. Chem.*, 1994, **33**, 1249; H. Stratemeier, B. Wagner, E. R. Krausz, R. Linder, H.-H. Schmidtke, J. Pebler, W. E. Hatfield, L. ter Haar, D. Reinen and M. A. Hitchman, *Inorg. Chem.*, 1994, **33**, 2320; T. Astley, P. J. Ellis, H. C. Freeman, M. A. Hitchman, F. R. Keene and E. R. T. Tiekink, *J. Chem. Soc.*, *Dalton Trans.*, 1995, 595; T. Astley, H. Headlam, M. A. Hitchman, F. R. Keene, J. Pilbrow, H. Stratemeier, E. R. T. Tiekink and Y. C. Zhong, *J. Chem. Soc.*, *Dalton Trans.*, 1995, 3809.
6 J. C. A. Boeyens, S. M. Dobson and R. D. Hancock, *Inorg. Chem.*, 1985, **24**, 3073; W. N. Setzer, C. A. Ogle, G. S. Wilson and R. S. Glass, *Inorg. Chem.*, 1983, **22**, 266.
7 M. Stebler and H. B. Bürgi, *J. Am. Chem. Soc.*, 1987, **109**, 1395; J. H. Ammeter, H. B. Bürgi, E. Gamp, V. Meyer-Sandrin and W. P. Jensen, *Inorg. Chem.*, 1979, **18**, 733.
8 K. Prout, A. Edwards, V. Mtetwa, J. Murray, J. F. Saunders and F. J. C. Rossotti, *Inorg. Chem.*, 1997, **36**, 2820.
9 W. Li, M. M. Olmstead, D. Miggins and R. H. Fish, *Inorg. Chem.*, 1996, **35**, 51 and refs. therein.
10 S. Trofimenko, *Chem. Rev.*, 1993, **93**, 943.
11 M. Itoh, K. Motoda, K. Shindo, T. Kamiusuki, H. Sakiyama, N. Matsumoto and H. Okawa, *J. Chem. Soc.*, *Dalton Trans.*, 1995, 3635; N. Sakagami, M. Nakahanada, K. Ino, A. Hioki and S. Kaizaki, *Inorg. Chem.*, 1996, **35**, 683; V. P. Hanot, T. D. Robert, J. Kolnaar, J. P. Haasnoot, J. Reedijk, H. Kooijman and A. L. Spek, *J. Chem. Soc.*, *Dalton Trans.*, 1996, 4275.
12 J. R. Backhouse, H. M. Lowe, E. Sinn, S. Suzuki and S. Woodward, *J. Chem. Soc.*, *Dalton Trans.*, 1995, 1489.
13 TEXRAY, Structure Analysis Package, Molecular Structure Corporation, Houston, TX, 1985.
14 ORTEP-3 for Windows, L. J. Farrugia, *J. Appl. Crystallogr.*, 1997, **30**, 565.
15 Values for ΔU_{obs} and e.s.d.s were calculated on a PC using the QBASIC program DELTA-U.
16 E. S. Ardiwinata, D. C. Craig and D. J. Phillips, *Inorg. Chim. Acta*, 1989, **166**, 233.
17 K. Nakamoto, *Infrared and Raman Spectra of Inorganic and Coordination Compounds*, John Wiley & Sons, New York, 4th edn., 1986.
18 A. B. P. Lever, *Inorganic Electronic Spectroscopy*, Elsevier, Amsterdam, 2nd edn., 1984.
19 B. N. Figgis and J. Lewis, *Prog. Inorg. Chem.*, 1964, **6**, 37.

Paper 8/09046G